Impaired phloem loading in genome-edited triple *knock-out* mutants of SWEET13 sucrose transporters

Margaret Bezrutczyk[1,2], Thomas Hartwig[1,2], Marc Horshman[2], Si Nian Char[3], Jinliang Yang[4], Bing Yang[3], Wolf B. Frommer[1,2, §] and Davide Sosso[2]

[1] Institute for Molecular Physiology, Heinrich Heine University Düsseldorf, and Max Planck Institute for Plant Breeding Research, Cologne, Germany

[2] Department of Plant Biology, Carnegie Science, 260 Panama St., Stanford, CA 94305, USA

[3] Department of Genetics, Development, and Cell Biology, Iowa State University, Ames, IA 50011, USA

[4] Department of Agronomy and Horticulture, University of Nebraska-Lincoln, Lincoln, NE 68588, USA

[§] For correspondence: frommew@hhu.de; +49 2118114826

One Sentence Summary: Three *SWEET* sucrose transporter paralogs are necessary for phloem loading in maize.

Summary

Crop yield depends on efficient allocation of sucrose from leaves to seeds. In *Arabidopsis*, phloem loading is mediated by a combination of SWEET sucrose effluxers and subsequent uptake by SUT1/SUC2 sucrose/H^+ symporters. ZmSUT1 is essential for carbon allocation in maize, but the relative contribution to apoplasmic phloem loading and retrieval of sucrose leaking from the translocation path is not known. We therefor tested whether SWEETs are important for phloem loading in maize.

Here we identified three leaf-expressed *SWEET* sucrose transporters as key components of apoplasmic phloem loading in *Zea mays* L. Notably, *ZmSWEET13* paralogs (*a*, *b, c*) are among the highest expressed genes in the leaf vasculature. Genome-edited triple *knock-out* mutants are severely stunted. Photosynthesis of mutants was impaired and leaves accumulated starch and soluble sugars. RNA-seq revealed profound transcriptional deregulation of genes associated with the photosynthetic apparatus and carbohydrate metabolism. GWAS analyses may indicate that variability in *ZmSWEET13s* is correlated with agronomical traits, specifically flowering time and leaf angle.

This work provides support for cooperation of three ZmSWEET13s with ZmSUT1 in phloem loading in *Zea mays* L. Our study highlights these three ZmSWEET13 sucrose transporters as possible candidates for the engineering of crop yield.

Keywords: corn, efflux, export, leaf, phloem loading, maize, sucrose, transport

Introduction

Crop yield is critical for human nutrition, yet the underlying machinery that ultimately determines yield potential is still not understood. Crop productivity under ideal conditions is determined by the efficiency with which plants intercept light, convert it into chemical energy, translocate photosynthates, and convert these to storage products in harvestable organs (Zhu *et al.*, 2010). In many crops, sucrose is the primary form for translocation inside the conduit (the phloem). A combination of SWEET-mediated efflux from phloem parenchyma and subsequent secondary active sucrose import by SUT sucrose/H^+ symporters is thought to create the driving force for pressure gradient-driven phloem transport and retrieval of sucrose leaking along the translocation path (Chen *et al.*, 2015a).

There is a debate regarding the mechanisms of phloem loading in crops. Sucrose is thought to follow one of three routes: (i) apoplasmic loading via plasma membrane transporters, (ii) symplasmic loading via diffusion through plasmodesmata, or (iii) polymer trapping via enzymatic addition of galactinol, which is thought to impair back-diffusion through plasmodesmata (Turgeon & Wolf, 2009; Chen *et al.*, 2015a). Some mechanisms may coexist, as suggested by anatomical studies which have found thin and thick walled sieve tubes in monocots, cell types that may differ regarding the primary loading mechanism (Botha, 2013).

In *Arabidopsis*, a SWEET/SUT-mediated apoplasmic mechanism appears important for phloem loading (Chen *et al.*, 2012, 2015a). SWEETs are a class of seven transmembrane helix transporters that function as hexose or sucrose uniporters (Xuan *et al.*, 2013). Multiple SemiSWEETs and SWEETs have been crystallized, and AtSWEET13 has been proposed to function in complexes via a 'revolving door' mechanism to accelerate transport efficacy (Feng & Frommer, 2015; Latorraca *et al.*, 2017; Han *et al.*, 2017). In Arabidopsis, SWEET roles include phloem loading, nectar secretion, pollen nutrition, and seed filling (Chen *et al.*, 2012; Sun *et al.*, 2013; Lin *et al.*, 2014; Sosso *et al.*, 2015). In rice, cassava, and cotton, SWEETs act as susceptibility factors for pathogen infections (Chen *et al.*, 2010; Cohn *et al.*, 2014; Cox *et al.*, 2017). AtSWEET11 and 12 are likely responsible for effluxing sucrose from the phloem

31 parenchyma into the apoplasm (Chen *et al.*, 2012). Sucrose is subsequently loaded
32 against a concentration gradient into the SECC via the SUT1 sucrose/H^+ symporter
33 (a.k.a. AtSUC2), powered by the proton gradient created by co-localized H^+/ATPases
34 (Riesmeier *et al.*, 1994; Gottwald *et al.*, 2000; Slewinski *et al.*, 2009; Srivastava *et al.*,
35 2009). Though the fundamental involvement of SUT transporters in phloem loading has
36 been demonstrated using RNAi and knock-out mutants in *Arabidopsis* (also in potato,
37 tobacco, tomato, and maize (Riesmeier *et al.*, 1994; Bürkle *et al.*, 1998; Srivastava *et*
38 *al.*, 2009; Chen *et al.*, 2015a), *atsweet11,12* and *atsuc2 (sut1)* mutants only showed
39 partially impaired phloem loading.

40 In monocots, including all cereal crops, the situation is less clear. In maize, the phloem-
41 expressed ZmSUT1 (Baker *et al.*, 2016) (phylogenetically in the SUT2 clade) appears to
42 be critically important for phloem translocation (Slewinski *et al.*, 2009), whereas rice
43 *ossut1* mutants and RNAi lines had no apparent growth or yield defects (Ishimaru *et al.*,
44 2001; Scofield *et al.*, 2002; Eom *et al.*, 2012). As a result, there is an ongoing debate
45 regarding the mechanisms behind phloem loading in cereals (Braun *et al.*, 2014; Regmi
46 *et al.*, 2016).

47 Here we identified a set of three close paralogs of SWEET13 from *Z. mays* L. as
48 essential sucrose transporters for phloem loading.

Material and Methods

Plant material and growth conditions

zmsweet13a, *zmsweet13b* and *zmsweet13c* alleles were obtained with a CRISPR-Cas9 construct targeting a sequence (5'-GCATCTACAAGAGCAAGTCGACGG-3', the underlined CGG for PAM) conserved in all three paralogs in the 3rd exon as described (Char *et al.*, 2017). T0 plants were selfed or outcrossed to B73 and plants which did not contain the CRISPR construct were selected for further analysis. T1, T2, and T3 plants homozygous for all three mutated genes (*zmsweet13abc*) were selected along with wild-type siblings. Height was assessed by weekly measurement from the soil surface to the top of the highest fully-developed leaf. Wild-type "siblings" were descendants of the Hi-II plants transformed and outcrossed once to B73, which in the T1 generation did not carry the CRISPR-Cas9 construct or any detectable mutations. Triple mutant plants either descended from selfed T0 Hi-II plants or outcrossed once to B73. The mutant phenotype was unaffected by the genetic difference. Mutants and wild-type plants were grown side by side, in greenhouses under long-day conditions (16h day/8h night, 28-30℃), and in 2016 in a summer field at Carnegie Science (Stanford, California, USA).

Genotyping of rice and maize plants

Genomic DNA was extracted from leaves using a Qiagen Biosprint 96. PCR was performed with the Terra PCR Direct Red Dye Premix Protocol (Clontech Laboratories) with melting temperatures of 60 °C, 64 °C, and 62.5 °C for *ZmSWEET13a*, *b*, and *c,* respectively (for primers see Table S2). Amplicons of relevant regions of the CRISPR-Cas9 targeted *ZmSWEET13* alleles were sequenced by Sequetech (Mountain View, CA). Chromatograms were analyzed using 4Peaks (www.nucleobytes.com/4peaks/).

Plastic embedding and sectioning

Flag leaves collected at 7:00 am were placed in 0.1 M cacodylate buffered fixative with 2% paraformaldehyde and 2% glutaraldehyde, vacuum infiltrated for 15 min and incubated overnight. Sample dehydration was performed by a graded ethanol series (10%, 30%, 50%, 70% and 95%). Sample embedding was performed according to the LR White embedding kit protocol (Electron Microscopy Science). Cross-sections (1.5

78 µm) were obtained on an Ultracut (Reichert), stained 30s with 0.1% toluidine blue and
79 washed with ddH_2O (2x), followed by 5 min of starch staining with saturated Lugol's
80 solution. Sections were mounted with CytoSeal 60 (EM Science).

81 **Phylogenetic analyses**

82 The evolutionary history was inferred by using Maximum Likelihood with a JTT matrix-
83 based model. The tree with the highest log likelihood (-3000.1) is shown. The
84 percentage of trees in which associated taxa clustered together is shown next to the
85 branches. Initial tree(s) for the heuristic search were obtained by Neighbor-Joining to a
86 matrix of pairwise distances with the JTT model used for estimation. The analysis
87 involved 16 polypeptides sequences. A minimum of 95% site coverage was required so
88 that no more than 5% alignment gaps, missing data, and ambiguous bases were
89 allowed at any position. There were a total of 252 positions in the final dataset.
90 Evolutionary analyses were conducted in MEGA6.

91 **Soluble sugar analyses**

92 Flag leaves were harvested from mature plants at 7:00 am. 70 mg of liquid nitrogen-
93 ground tissue was incubated for 1 hour with 1 ml of 80% ethanol on ice with frequent
94 mixing. Samples were spun for 5 min at 4 °C at 13,000 *g*, and supernatant was
95 removed. This step was repeated once. The liquid supernatant was subsequently dried
96 in a vacuum concentrator and re-suspended in water. Sucrose, glucose and fructose
97 were measured using NAD(P)H-coupled enzymatic methods using a plate reader
98 M1000 (Tecan), with measured values normalized to fresh weight. Starch quantification
99 was performed as previously described (Sosso *et al.*, 2015).

100 **Starch staining**

101 Flag leaves collected at 7:00 am were were boiled in 95% ethanol for approximately 30
102 min (until chlorophyll pigments disappeared). Cleared leaves were submerged in
103 saturated Logol's iodine (IKI) solution for 15 min, rinsed twice with H_2O, and imaged
104 with a Lumix GF1 camera (Panasonci, Kadoma, Osaka, Japan). The IKI solution used
105 for starch staining was made by adding 1 g of iodine and 1 g of Potassium Iodide to 100
106 mL H_2O.

107 **RNA isolation and transcript analyses**

108 RNA was extracted using the Trizol method (Invitrogen). First strand cDNA was
109 synthesized using Quantitect reverse transcription Kit (Qiagen). qRT-PCR to determine
110 expression level was performed using the LightCycler 480 (Roche), and the $2^{-\Delta Ct}$
111 method for relative quantification. Wild-type maize and *zmsweet13abc* flag leaves were
112 sampled at 5:00 pm. Primers in the last exon and the 3′ UTR of *ZmSWEET13a, b,* and *c*
113 (Supplementary Table 2) were used for qRT-PCR to determine gene expression levels.
114 Internal references were *Zm18s* and *ZmLUG***.**

115 **FRET sucrose sensor analysis in HEK293T cells**

116 *ZmSWEET13a, b,* and *c* coding sequences were cloned into the Gateway entry vector
117 pDONR221f1, followed by LR recombination into pcDNA3.2V5 for expression in
118 HEK293T cells. HEK293T cells were co-transfected with *ZmSWEET13a, b,* or *c* in
119 *pcDNA3.2V5* and the sucrose sensor FLIPsuc90μΔ1V (Chen *et al.*, 2012) using
120 Lipofectamine 2000 (Invitrogen). For FRET imaging, HBSS medium was used to
121 perfuse HEK293T/FLIPsuc90μΔ1V cells with defined pulses containing 20 mM sucrose
122 in buffer. Image acquisition and analysis were performed as previously described (Chen
123 *et al.*, 2012). AtSWEET12 was used as a positive control. Negative control were empty
124 vector transfectants.

125 **Transient gene expression in *Nicotiana benthamiana* leaves**

126 The *Agrobacterium tumefaciens* strain GV3101 was transformed with the binary
127 expression clone (pAB117) carrying *ZmSWEET13a*, *b*, or *c* C-terminally fused with
128 eGFP and driven by the CaMV 35S promoter. Agrobacterium culture and tobacco leaf
129 infiltration were performed as described (Sosso *et al.*, 2015). Chloroplast
130 autofluorescence was detected on a Leica TCS SP8 confocal microscope (470 nm
131 excitation with simultaneous 522–572 nm (eGFP) and 667–773 nm emission
132 (autofluorescence)). Epidermal leaf chloroplast autofluorescence (Dupree *et al.*, 1991)
133 allowed us to determine eGFP vacuolar localization (surrounding the chloroplasts) and
134 plasma membrane localization was deduced (adjacent to chloroplasts; according to
135 bright-field image). Image analysis done using Fiji software (https://fiji.sc/).

136 **Analyses of photosynthetic rates**

137 Licor LI-6800 measurements were taken at mid-day under normal greenhouse
138 conditions (28 °C, PAR 1000, 60% relative humidity). 2 cm diameter disc of leaf was
139 clamped inside the Licor measurement chamber and relative levels of CO_2 inside and
140 outside of the chamber were measured, with μmol $m^{-2}s^{-1}$ CO_2 absorbed by leaf
141 segment inside chamber used as a proxy for photosynthesis rate. Measurements were
142 made at the tips of Leaf 7 - Leaf 10 at mid-day.

143 **Candidate gene association study**

144 To test whether sequences at SWEET loci are associated with phenotypic variations in
145 the maize population, we analyzed the maize diversity panel composed of 282 inbred
146 lines (HapMap3 SNP data (Bukowski *et al.*, 2015) for the panel from the Panzea
147 database (www.panzea.org)). We filtered SNP data (MAF > 0.1; missing rate < 0.5)
148 using PLINK (Purcell *et al.*, 2007) and calculated a kinship matrix using GEMMA (Zhou
149 & Stephens, 2012) using the filtered SNP set. GWAS was performed by fitting a mixed
150 linear model using GEMMA, where the kinship matrix was fitted as random effects in the
151 model. An FDR approach (Benjamini & Hochberg, 1995) was employed to control the
152 multiple test problem with a cutoff of 0.05. Linkage disequilibrium of SNPs in our
153 candidate genes with significant association SNPs was calculated using PLINK (Purcell
154 *et al.*, 2007).

155 **RNA-seq and data analysis**

156 *zmsweet13abc* triple mutants and WT siblings were grown in soil under greenhouse
157 conditions. Total RNA was isolated from flag leaf tissues using acidic phenol extraction
158 as described previously (Eggermont *et al.*, 1996). Purification of poly-adenylated mRNA
159 using oligo(dT) beads, construction of barcoded libraries, and sequencing using Illumina
160 HiSeq technology (150 bp paired-end reads) were performed by Novogene
161 (https://en.novogene.com/) using manufacturer recommendations. Trimmed and QC-
162 filtered sequence reads were mapped to the B73 AGPv3 genome using STAR (v. 2.54)
163 (Dobin *et al.*, 2013) in two pass mode (parameters: --outFilterScoreMinOverLread 0.3, --
164 outFilterMatchNminOverLread 0.3, --outSAMstrandField intronMotif, --outFilterType
165 BySJout, --outFilterIntronMotifs RemoveNoncanonical, --quantMode TranscriptomeSAM

166 GeneCounts). Unique reads were filtered by mapping quality (q20) and PCR duplicates
167 removed using Samtools (v. 1.3.1). Gene expression was analyzed in R (v. 3.4.1) using
168 DEseq2 software (v. 1.16.1) (Love *et al.*, 2014). Genes were defined as differentially
169 expressed by a two-fold expression difference with a p-value, adjusted for multiple
170 testing, of < 0.05. Accession numbers for the RNA-Seq data in the Gene Expression
171 Omnibus database will be made available.

172 **Results**

173 To directly test whether SWEETs are involved in phloem loading in maize, we evaluated
174 the role of leaf-expressed maize *SWEETs* in carbon allocation. We identified three
175 *SWEET13* paralogs (GRMZM2G173669: *ZmSWEET13a*, GRMZM2G021706:
176 *ZmSWEET13b*, GRMZM2G179349: *ZmSWEET13c*) as the most highly expressed
177 SWEETs in maize leaves (**Fig. S1**). *ZmSWEET13a* and *b* are located in tandem on
178 chromosome 10 in a region syntenic with the *OsSWEET13* locus in rice, while
179 *ZmSWEET13c* is on chromosome 3 (**Fig. S2**). Interestingly, maize appeared to be one
180 of few cereals carrying three *SWEET13* paralogs in its genome, along with *S. bicolor*
181 and *T. urartu* (**Figure 1a; Fig. S3**). *ZmSWEET13a, b* and *c* are preferentially expressed
182 in bundle sheath/vein preparations rather than mesophyll (**Fig. S4**), as is *ZmSUT1*.
183 ZmSUT1 and the three SWEETs showed higher expression in leaf tips (**Fig. S5**). We
184 tested the transport activity of the three SWEETs by coexpressing each with sucrose
185 FRET (Förster resonance energy transfer) sensors in human HEK293T cells (Chen *et*
186 *al.*, 2010, 2012). All three SWEETs mediated sucrose transport in mammalian cells
187 (**Fig. 1b**). To test whether these SWEETs were part of (i) intercellular translocation or
188 (ii) intracellular sugar sequestration similar to the *Arabidopsis* SWEET2, 16 or 17
189 (Chardon *et al.*, 2013; Klemens *et al.*, 2013; Guo *et al.*, 2014; Chen *et al.*, 2015b), we
190 tested their subcellular localization in transiently transformed tobacco cells, and found
191 that they localized preferentially to the plasma membrane (**Fig. 1c**).

192 Recently, *ZmSWEET13* had been implicated as a possible key player in C4-
193 photosynthesis in grasses (Emms *et al.*, 2016). To test their role in maize, we designed
194 guide RNAs that target a conserved region within a transmembrane domain, assuming
195 that such mutations would lead to complete loss of function. We generated single
196 *knock-out* mutants, as well as combinations of mutant alleles, using CRISPR-Cas9 (**Fig.**
197 **S6**). Genome editing allowed us to recover two mutant alleles of *ZmSWEET13a*, four of
198 *ZmSWEET13b* and three for *ZmSWEET13c*. The majority of mutations were caused by
199 single nucleotide insertions in the target sequence. All mutations create premature
200 STOP codons leading to truncated polypeptides (at amino acid 129 in the fourth of
201 seven transmembrane domains) (**Fig. S6**). T2 lines carrying homozygous mutations in
202 all three genes were characterized by severe growth defects (**Fig. 2a**). The growth

203 phenotype was verified in subsequent generations in the greenhouse and a single field
204 season. Single and double mutants showed slight growth defects, while triple mutants
205 showed substantial defects: plants were severely stunted with shorter, narrower leaves
206 (**Fig. 2a-c**). Leaves were chlorotic, accumulated 5x more starch and 4x more soluble
207 sugars compared to wild-type (**Fig. 3a-c**), likely a consequence of impaired phloem
208 loading. Accumulation of sugars and starch occurred primarily in mesophyll and bundle
209 sheath cells and strongly impacted photosynthesis, even in greenhouse-grown mutant
210 plants (**Fig. 3d, e; Fig. S7**). In the field, triple mutants from five independent allelic
211 combinations presented even more severe phenotypes, with extreme chlorosis,
212 massive anthocyanin accumulation and extremely stunted growth; in several cases
213 resulting in lethality (**Fig. S8**). *SWEET13* mRNA levels were drastically reduced in all
214 three *ZmSWEET13s*, as quantified by RNA-seq and qRT-PCR (**Fig. S9** and **Fig. 2d**). In
215 summary, the strong phenotype of the triple mutant is consistent with maize using
216 predominantly an apoplasmic phloem loading mechanism.

217 Despite the severe defects, triple mutant plants grown in the greenhouse (as well as a
218 subset in the field) exported sufficient sugars from leaves to produce viable seeds. A
219 possible explanation for the viability of the triple mutants could be compensation by
220 other sucrose-transporting clade III SWEETs. To test this hypothesis and to obtain
221 insights about possible physiological changes in the mutants, we performed an RNA-
222 seq on flag leaves of wild-type (Hi-II outcrossed once to B73) and triple mutant plants
223 (Hi-II background). Notably, we did not observe significant enrichment of mRNA of clade
224 III *SWEETs*, arguing against transcriptional compensation by other clade III *SWEETs*
225 (**Fig. S9**). Consistent with impaired photosynthesis and chlorosis, mRNA levels of
226 multiple genes encoding functions in the light harvesting complex and
227 chlorophyll/tetrapyrrole biosynthesis were substantially reduced in triple mutants (**Fig.
228 S10** and **Fig. S11**). Furthermore, in line with the accumulation of starch and soluble
229 sugars in leaves, we found that transcripts related to carbohydrate synthesis and
230 degradation were affected in the triple mutants (**Fig. S12**).

231 A recent study has found that the *Arabidopsis* homolog AtSWEET13 (although
232 phylogenetically not the closest homolog of ZmSWEET13) can also transport the plant
233 hormone gibberellin (Kanno *et al.*, 2016). The observed phenotypes for the triple

234 zm*sweet13 knock out* mutants in maize are consistent with a primary role in sucrose
235 transport and distinct from the ones observed in the *Arabidopsis sweet13;14* double
236 mutant; i.e., male sterility, increased seedling and seed size (Kanno *et al.*, 2016).

237 To determine if variation in the *ZmSWEET13* genes may account for differences in
238 agronomically important traits in existing maize lines, we conducted a genome-wide
239 association study (GWAS) using phenotypic traits obtained from maize diversity panel
240 (Flint-Garcia *et al.*, 2005). We obtained genotypic data from maize HapMap3 SNPs
241 (Bukowski *et al.*, 2015) and filtered out SNPs having minor allele frequency < 0.1 and
242 missing rate > 0.5, leaving ~13 million SNPs for analyses. We performed GWAS using a
243 mixed linear model approach (Zhou & Stephens, 2012), where kinship calculated from
244 the genome-wide SNPs was fitted as the random effects. The SNPs that passed the
245 FDR threshold of 0.05 and showed linkage disequilibrium (R^2 > 0.8) with *ZmSWEET13s*
246 genes were considered significant associations. SNPs in *ZmSWEET13s* were
247 significantly associated with ear-related traits (i.e. ear rank number and ear height) and
248 developmental traits (i.e. days to silk, days to tassel, middle leaf angle, and germination
249 count) (**Fig. S13** and **Fig. S14**). While these results are compatible with a key role of
250 *ZmSWEET13s* in carbon allocation, it will be necessary to determine whether
251 polymorphisms in these genes or flanking regions are causative for these traits.

252 **Discussion**

253 Phloem sap of many monocots and dicots contains very high sucrose concentrations,
254 and it is thought that this gradient creates the drive for phloem translocation of sucrose
255 and all other molecules in the phloem sap. Inhibition of the production of the SUT1
256 protein, by RNAi or mutations, typically leads to stunted growth and accumulation of
257 carbohydrates in leaves (Riesmeier *et al.*, 1994; Bürkle *et al.*, 1998). Chlorosis and
258 inhibition of photosynthesis, which often accompany the general growth defects, may
259 either be due to feedback inhibition of photosynthesis or may be a consequence of
260 nutrient deficiencies caused by the reduced supply of carbohydrates to the root system
261 (Ainsworth & Bush, 2011). SUTs function as sucrose/H^+ symporters and appear to fulfill
262 two roles: (i) loading of the SECC with sucrose in source leaves, and (ii) retrieval of
263 sucrose that diffuses out of the SECC as a consequence of the high sucrose
264 concentration in the SECC relative to surrounding tissues. SUTs import sucrose from
265 the cell wall space, implying the existence of transporters that efflux sucrose into the cell
266 wall space preceding uptake by SUTs. AtSWEET11 and 12 are candidates for this role
267 in *Arabidopsis*: they appear to function as uniporters and can thus serve as cellular
268 efflux systems. Both SWEETs were highly expressed in leaves, localize to the phloem
269 parenchyma, and *atsweet11;12* mutants were smaller and accumulated starch in
270 leaves. However, the phenotype was relatively weak, implying leaky mutations,
271 compensation by other transporters, or the coexistence of other phloem loading
272 mechanisms. Other mechanisms could include symplasmic transport, or yet unknown
273 processes. Lastly, is possible that SUTs play a major role in sucrose retrieval along the
274 path in addition to their role in phloem loading, while ZmSWEET13's are thought to be
275 only involved in sucrose efflux prior to SUT1 uptake into phloem. Would a mutant of
276 *ZmSWEET13* present weak defects similar to those in *atsweet11;12* plants, or a more
277 severe phenotype equivalent that in *zmsut1* mutants?
278 Here, we show that maize has three paralogs in clade III of the SWEET family that are
279 among the most highly expressed genes in leaf tissue. They derive from relatively
280 recent gene duplication events: sorghum and wheat have three copies per genome,
281 while Brachypodium and rice each have only one. The comparatively high number of
282 *SWEET13s* had been attributed to specific roles in C4 photosynthesis, however the

283 presence of three *SWEET13s* in wheat puts this interpretation into question. Evidence
284 that the maize SWEET13s cooperate in phloem loading is based on two key
285 observations: a severe growth defect similar to that of *zmsut1* mutants, and massive
286 accumulation of free sugars and starch in leaves. These phenotypic effects are also
287 similar to the RNAi phenotypes in potato and tobacco (Riesmeier *et al.*, 1994; Bürkle *et*
288 *al.*, 1998). The observed growth defect in maize is much more severe than that of the
289 *atsweet11;12* mutant in *Arabidopsis,* and comparable to that of the *zmsut1* mutant
290 (Slewinski *et al.*, 2009; Chen *et al.*, 2012). We thus propose that the three
291 ZmSWEET13s and ZmSUT1 play dominant roles in phloem loading.
292 It is noteworthy, that the combined *zmsweet13abc* mutations are not lethal, since the
293 plants still produce fertile viable offspring, implying additional mechanisms for phloem
294 loading in maize. While it is possible that other transporters might compensate, it is
295 unlikely that other SWEETs take over such roles, as judged by the lack of induction of
296 other clade III SWEET genes in the mutants. Therefore, maize likely uses either
297 symplasmic or other loading mechanisms in parallel.
298 It is still not clear whether *SWEET13* triplication mainly serves to increase the amount of
299 SWEET proteins in the same cells (e.g. phloem parenchyma), or if each SWEET13
300 transporter mediates efflux from a specific cell type and loading is achieved in a multi-
301 tier fashion. This question is of particular interest because *in situ* hybridization
302 experiments identified SUT1 in companion cells, xylem and phloem parenchyma, as
303 well as the bundle sheath. To address this question, we generated translational reporter
304 gene fusions and included the first three introns. However GUS activity or GFP
305 fluorescence were not detectable in any of the transformants carrying fusions for any of
306 the three SWEET13s (data not shown). We therefore hypothesize that additional
307 elements are required for proper expression of these constructs.
308 Another interesting question is whether maize can serve as a model for phloem loading
309 in rice, barley and wheat. Surprisingly, RNAi of the rice homolog of *ZmSUT1* did not
310 lead to a detectable effect on the phenotype of the sporophyte (Ishimaru *et al.*, 2001).
311 Thus, it remains a matter of debate whether rice uses predominantly apoplasmic and
312 symplasmic or other mechanisms simultaneously. It will therefore be important to study
313 the role of SWEET homologs in rice and other crops. It is noteworthy in this context that

314 OsSWEET11 and 15 are expressed preferentially in the caryopsis and act as key
315 players in apoplasmic unloading processes in developing rice grains (Yang, parallel
316 submission)(Ma *et al.*, 2017).
317 Finally and most importantly, it will be interesting to see whether overexpression of
318 clade III SWEETs in leaves of cereals may help to increase yield potential.
319

Acknowledgments

We thank Joelle Sasse, Bi-Huei Hou, Aurélie Grimault, Franklin Talavera-Rauh, Xiao-Qing Xu, Grayson Badgley and Guido Grossmann for experimental support during various analyses. We thank Ari Kornfeld (Dep. Global Ecology, Carnegie Science) for help and advice in photosynthesis measurements. This work was made possible by research grants from Syngenta Crop Protection, LLC (WBF), the Office of Basic Energy Sciences of the US Department of Energy (DE-FG02-04ER15542; WBF), and the National Science Foundation (IOS-1258018; BY, WBF). WF's lab is supported by the Alexander von Humboldt Foundation.

Author Contributions

MB, SNC, BY, WBF and DS conceived and designed experiments. MB, MH, TH, SNC, DL, BL and DS performed experiments. MB, TH, BY, WBF and DS analyzed the data. DS and WBF wrote the manuscript, MB and BY helped with revisions.

Competing Financial Interests

The authors (DS and WBF, on behalf of Carnegie Science) have filed a PCT patent application based in part on this work with the US Patent and Trademark Office.

References

Ainsworth EA, Bush DR. **2011**. Carbohydrate Export from the Leaf: A Highly Regulated Process and Target to Enhance Photosynthesis and Productivity. *Plant Physiology* **155**: 64.

Baker RF, Leach KA, Boyer NR, Swyers MJ, Benitez-Alfonso Y, Skopelitis T, Luo A, Sylvester A, Jackson D, Braun DM. **2016**. Sucrose transporter ZmSut1 expression and localization uncover new insights into sucrose phloem loading. *Plant Physiology* **172**: 1876–1898.

Benjamini Y, Hochberg Y. **1995**. Controlling the false discovery rate: a practical and powerful approach to multiple testing. *Journal of the Royal Statistical Society. Series B (Methodological)* **57**: 289–300.

Botha CEJ. **2013**. A tale of two neglected systems-structure and function of the thin- and thick-walled sieve tubes in monocotyledonous leaves. *Frontiers in Plant Science* **4**: 297.

Braun DM, Wang L, Ruan Y-L. **2014**. Understanding and manipulating sucrose phloem loading, unloading, metabolism, and signalling to enhance crop yield and food security. *Journal of Experimental Botany* **65**: 1713–1735.

Bukowski R, Guo X, Lu Y, Zou C, He B, Rong Z, Wang B, Xu D, Yang B, Xie C, *et al.* 2015. Construction of the third generation *Zea mays* haplotype map. *bioRxiv*.

Bürkle L, Hibberd JM, Quick WP, Kühn C, Hirner B, Frommer WB. **1998**. The H^+-sucrose cotransporter NtSUT1 is essential for sugar export from tobacco leaves. *Plant Physiology* **118**: 59–68.

Char SN, Neelakandan AK, Nahampun H, Frame B, Main M, Spalding MH, Becraft PW, Meyers BC, Walbot V, Wang K, *et al.* 2017. An *Agrobacterium*-delivered CRISPR/Cas9 system for high-frequency targeted mutagenesis in maize. *Plant Biotechnology Journal* **15**: 257–268.

Chardon F, Bedu M, Calenge F, Klemens PA, Spinner L, Clement G, Chietera G, Leran S, Ferrand M, Lacombe B, *et al.* 2013. Leaf fructose content is controlled by the vacuolar transporter SWEET17 in *Arabidopsis*. *Current Biology* **23**: 697–702.

Chen L-Q, Cheung LS, Feng L, Tanner W, Frommer WB. **2015a**. Transport of sugars. *Annual Review of Biochemistry* **84**: 865–894.

Chen LQ, Hou BH, Lalonde S, Takanaga H, Hartung ML, Qu XQ, Guo WJ, Kim JG, Underwood W, Chaudhuri B, *et al.* 2010. Sugar transporters for intercellular exchange and nutrition of pathogens. *Nature* **468**: 527–32.

Chen H-Y, Huh J-H, Yu Y-C, Ho L-H, Chen L-Q, Tholl D, Frommer WB, Guo W-J. **2015b**. The *Arabidopsis* vacuolar sugar transporter SWEET2 limits carbon sequestration from roots and restricts *Pythium* infection. *The Plant Journal: For Cell and Molecular Biology*.

Chen LQ, Qu XQ, Hou BH, Sosso D, Osorio S, Fernie AR, Frommer WB. **2012**. Sucrose efflux mediated by SWEET proteins as a key step for phloem transport. *Science* **335**: 207–11.

Cohn M, Bart RS, Shybut M, Dahlbeck D, Gomez M, Morbitzer R, Hou B-H, Frommer WB, Lahaye T, Staskawicz BJ. **2014**. *Xanthomonas axonopodis* virulence is promoted by a transcription activator-like effector-mediated induction of a SWEET sugar transporter in cassava. *Molecular plant-microbe interactions: MPMI* **27**: 1186–1198.

Cox KL, Meng F, Wilkins KE, Li F, Wang P, Booher NJ, Carpenter SCD, Chen L-Q, Zheng H, Gao X, *et al.* 2017. TAL effector driven induction of a *SWEET* gene confers susceptibility to bacterial blight of cotton. *Nature Communications* **8**: 15588.

Dobin A, Davis CA, Schlesinger F, Drenkow J, Zaleski C, Jha S, Batut P, Chaisson M, Gingeras TR. **2013**. STAR: ultrafast universal RNA-seq aligner. *Bioinformatics* **29**: 15–21.

Dupree P, Pwee K-H, Gray JC. **1991**. Expression of photosynthesis gene-promoter fusions in leaf epidermal cells of transgenic tobacco plants. *The Plant Journal* **1**: 115–120.

Eggermont K, Goderis IJ, Broekaert WF. **1996**. High-throughput RNA extraction from plant samples based on homogenisation by reciprocal shaking in the presence of a mixture of sand and glass beads. *Plant Molecular Biology*: 273–279.

Emms DM, Covshoff S, Hibberd JM, Kelly S. **2016**. Independent and parallel evolution of new genes by gene duplication in two origins of C4 photosynthesis provides new insight into the mechanism of phloem loading in C4 species. *Molecular Biology and Evolution* **33**: 1796–1806.

Eom J-S, Choi S-B, Ward JM, Jeon J-S. **2012**. The mechanism of phloem loading in rice (*Oryza sativa*). *Molecules and Cells* **33**: 431–438.

Feng L, Frommer WB. **2015**. Structure and function of SemiSWEET and SWEET sugar transporters. *Trends in Biochemical Sciences* **40**: 480–486.

Flint-Garcia SA, Thuillet A-C, Yu J, Pressoir G, Romero SM, Mitchell SE, Doebley J, Kresovich S, Goodman MM, Buckler ES. **2005**. Maize association population: a high-resolution platform for quantitative trait locus dissection. *The Plant Journal* **44**: 1054–1064.

Gottwald JR, Krysan PJ, Young JC, Evert RF, Sussman MR. **2000**. Genetic evidence for the in planta role of phloem-specific plasma membrane sucrose transporters. *Proceedings of the National Academy of Sciences of the USA* **97**: 13979–84.

Guo W-J, Nagy R, Chen H-Y, Pfrunder S, Yu Y-C, Santelia D, Frommer WB, Martinoia E. **2014**. SWEET17, a facilitative transporter, mediates fructose transport across the tonoplast of *Arabidopsis* roots and leaves. *Plant Physiology* **164**: 777–789.

Han L, Zhu Y, Liu M, Zhou Y, Lu G, Lan L, Wang X, Zhao Y, Zhang XC. **2017**. Molecular mechanism of substrate recognition and transport by the AtSWEET13 sugar transporter. *Proceedings of the National Academy of Sciences of the United States of America*.

Ishimaru K, Hirose T, Aoki N, Takahashi S, Ono K, Yamamoto S, Wu J, Saji S, Baba T, Ugaki M, *et al.* 2001. Antisense expression of a rice sucrose transporter OsSUT1 in rice (*Oryza sativa* L.). *Plant & Cell Physiology* **42**: 1181–1185.

Kanno Y, Oikawa T, Chiba Y, Ishimaru Y, Shimizu T, Sano N, Koshiba T, Kamiya Y, Ueda M, Seo M. **2016**. AtSWEET13 and AtSWEET14 regulate gibberellin-mediated physiological processes. *Nature Communications* **7**: 13245.

Klemens PAW, Patzke K, Deitmer J, Spinner L, Le Hir R, Bellini C, Bedu M, Chardon F, Krapp A, Neuhaus HE. **2013**. Overexpression of the vacuolar sugar carrier AtSWEET16 modifies germination, growth, and stress tolerance in *Arabidopsis*. *Plant Physiology* **163**: 1338–1352.

Latorraca NR, Fastman NM, Venkatakrishnan AJ, Frommer WB, Dror RO, Feng L. **2017**. Mechanism of substrate translocation in an alternating access transporter. *Cell* **169**: 96–107.e12.

Lin IW, Sosso D, Chen L-Q, Gase K, Kim S-G, Kessler D, Klinkenberg PM, Gorder MK, Hou B-H, Qu X-Q, *et al.* 2014. Nectar secretion requires sucrose phosphate synthases and the sugar transporter SWEET9. *Nature* **508**: 546–549.

Love MI, Huber W, Anders S. **2014**. Moderated estimation of fold change and dispersion for RNA-seq data with DESeq2. *Genome Biology* **15**: 550.

Ma L, Zhang D, Miao Q, Yang J, Xuan Y, Hu Y. **2017**. Essential Role of Sugar Transporter OsSWEET11 During the Early Stage of Rice Grain Filling. *Plant & Cell Physiology* **58**: 863–873.

Purcell S, Neale B, Todd-Brown K, Thomas L, Ferreira MAR, Bender D, Maller J, Sklar P, de Bakker PIW, Daly MJ, *et al.* 2007. PLINK: a tool set for whole-genome association and population-based linkage analyses. *The American Journal of Human Genetics* **81**: 559–575.

Regmi KC, Zhang S, Gaxiola RA. **2016**. Apoplasmic loading in the rice phloem supported by the presence of sucrose synthase and plasma membrane-localized proton pyrophosphatase. *Annals of Botany* **117**: 257–268.

Riesmeier JW, Willmitzer L, Frommer WB. **1994**. Evidence for an essential role of the sucrose transporter in phloem loading and assimilate partitioning. *The EMBO Journal* **13**: 1–7.

Scofield GN, Hirose T, Gaudron JA, Furbank RT, Upadhyaya NM, Ohsugi R. **2002**. Antisense suppression of the rice transporter gene, OsSUT1, leads to impaired grain filling and germination but does not affect photosynthesis. *Functional Plant Biology* **29**: 815–826.

Slewinski TL, Meeley R, Braun DM. **2009**. Sucrose transporter1 functions in phloem loading in maize leaves. *Journal of Experimental Botany* **60**: 881–892.

Sosso D, Luo D, Li Q-B, Sasse J, Yang J, Gendrot G, Suzuki M, Koch KE, McCarty DR, Chourey PS, *et al.* 2015. Seed filling in domesticated maize and rice depends on SWEET-mediated hexose transport. *Nature Genetics* **47**: 1489–1493.

Srivastava AC, Dasgupta K, Ajieren E, Costilla G, McGarry RC, Ayre BG. **2009**. *Arabidopsis* plants harbouring a mutation in AtSUC2, encoding the predominant sucrose/proton symporter necessary for efficient phloem transport, are able to complete their life cycle and produce viable seed. *Annals of Botany* **104**: 1121–1128.

Sun MX, Huang XY, Yang J, Guan YF, Yang ZN. **2013**. Arabidopsis RPG1 is important for primexine deposition and functions redundantly with RPG2 for plant fertility at the late reproductive stage. *Plant Reproduction* **26**: 83–91.

Turgeon R, Wolf S. **2009**. Phloem transport: cellular pathways and molecular trafficking. *Annual Review of Plant Biology* **60**: 207–221.

Xuan YH, Hu YB, Chen LQ, Sosso D, Ducat DC, Hou BH, Frommer WB. **2013**. Functional role of oligomerization for bacterial and plant SWEET sugar transporter family. *Proceedings of the National Academy of Sciences of the United States of America* **110**: E3685-94.

Zhou X, Stephens M. **2012**. Genome-wide efficient mixed-model analysis for association studies. *Nature Genetics* **44**: 821–824.

Zhu XG, Long SP, Ort DR. **2010**. Improving photosynthetic efficiency for greater yield. *Annual Review of Plant Biology* **61**: 235–61.

Figure 1. *ZmSWEET13* paralogs phylogeny, functional and subcellular characterization.

(A) Scheme of phylogenetic relationship between putative orthologs in grasses. Chronogram branch divergence time-points are in million years (Emms *et al.*, 2016).

(B) Sucrose transport activity by *ZmSWEET13a*, *b* and *c* in HEK293T cells coexpressing the FLIPsuc90μΔ1V (sucrose). Cell were transfected to express sensors only as negative control, or to co-express AtSWEET12 as positive controls for sucrose. HEK cells were subjected to a 20mM sucrose pulse for 3 minutes, (mean ± s.e.m., repeated independently four times with comparable results).

(C) Confocal images (Z-stack) of *Agrobacterium*-infiltrated *N. benthamiana* epidermal leaf cells. ZmSWEET13a-eGFP (C-term), as well b and c indicated localization at the plasma membrane. The eGFP signal (Green; 522–572 nm) was merged with fluorescence derived from chloroplasts (Blue; 667–773 nm). Fluorescence was visualized using confocal laser scanning microscopy, 3 days after *Agrobacterium* infiltration. Scale bars, 50 μm.

Figure 2. *ZmSWEET13* paralogs triple mutant characterization.

(A) Photograph of fully mature wild-type and same-age *zmsweet13a1b1c1* triple mutant, showing reduced growth and leaf chlorosis. Bar: 50 cm.

(B) Leaves comparison of plants presented in Fig. 2a, showing *zmsweet13a1b1c1* reduced growth and chlorosis.

(C) Height quantification throughout wild-type and triple mutant life cycle in the greenhouse (mean ± s.e.m., n=17 and 15).

(D) Relative expression (by qRT-PCR) of *ZmSWEET13* paralogs in maize flag leaf from wild-type and *zmsweet13abc*. Samples were harvested at 4:00 pm (mean ± s.e.m., n=3 technical replicates with expression normalized to 18S levels, repeated independently five times with comparable results).

Figure 3. *zmsweet13abc* starch and soluble sugar accumulation.

(A) Flag leaves were collected at dawn (7:00am), cleared with boiling ethanol and stained for 15 min with a saturated IKI (Lugol's solution).

(B) Starch quantification of leaves displayed in (A). The triple mutant shows 5x more starch in the leaf tip and blade, while no significant differences where measured in the sheath (mean ± s.e.m., n=3 technical replicates, repeated independently three times with comparable results).

(C) Soluble sugar measurements of wild-type and *zmsweet13a2b1c1* in maize flag leaf sections. The triple mutant shows higher sugar concentration in both the tip and the base of the leaf. Samples were harvested at 7:00 am (mean ± s.e.m., n=3 technical replicates, repeated independently three times with comparable results).

(D) Cross-sections of wild-type and triple mutant leaves harvested at the end of the night, fixed, embedded and stained with Lugol's solution for starch. Mutant *zmsweet13a2b1c1* accumulates high amounts of starch in both mesophyll and bundle sheath cells. Bar: 75 mm.

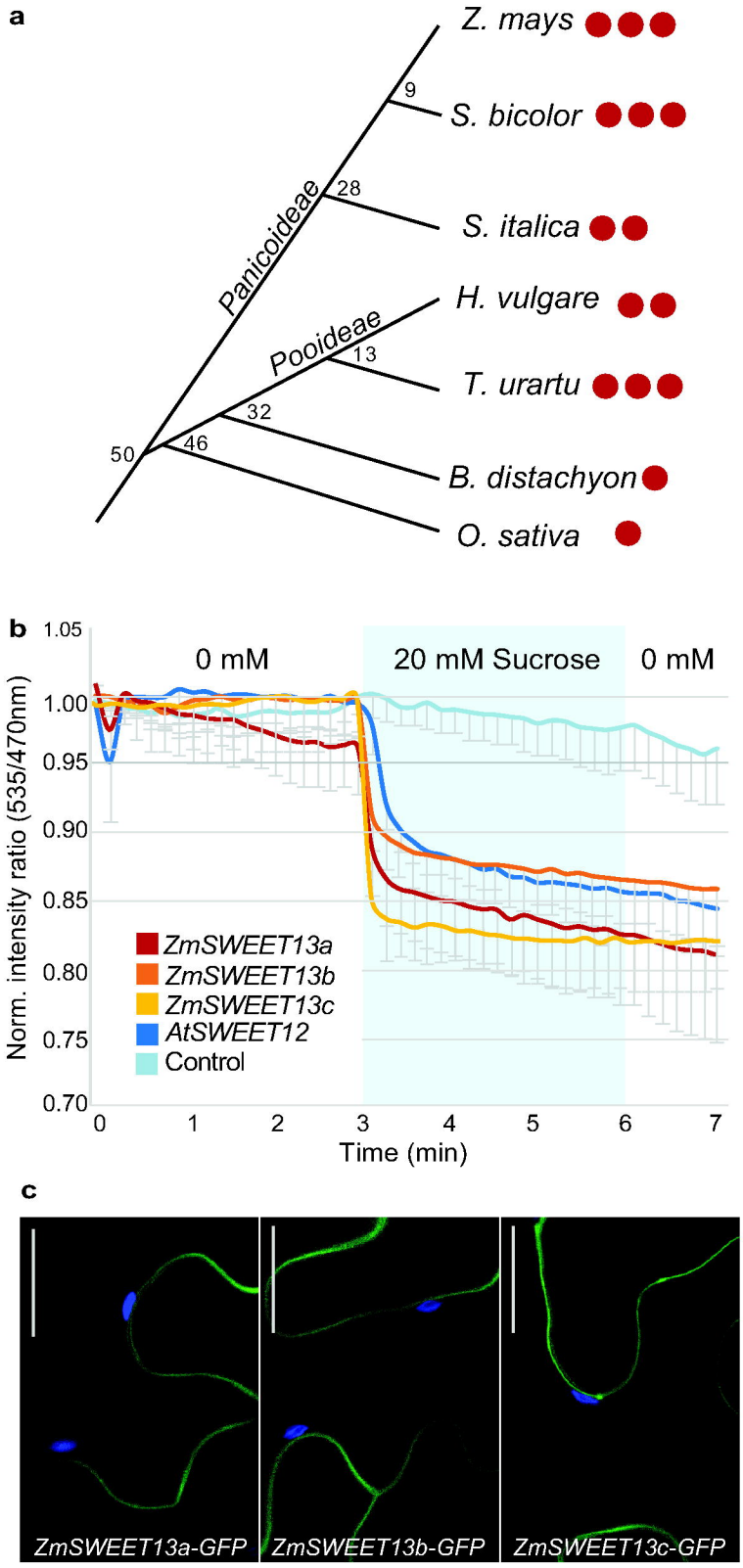
a
Z. mays
S. bicolor
S. italica
H. vulgare
T. urartu
B. distachyon
O. sativa
Panicoideae
Pooideae
9
28
13
32
46
50
b
0 mM
20 mM Sucrose
0 mM
Norm. intensity ratio (535/470nm)
1.05
1.00
0.95
0.90
0.85
0.80
0.75
0.70
0
1
2
3
4
5
6
7
Time (min)
ZmSWEET13a
ZmSWEET13b
ZmSWEET13c
AtSWEET12
Control
c
ZmSWEET13a-GFP
ZmSWEET13b-GFP
ZmSWEET13c-GFP

wild-type
zmsweet13a1b1c1

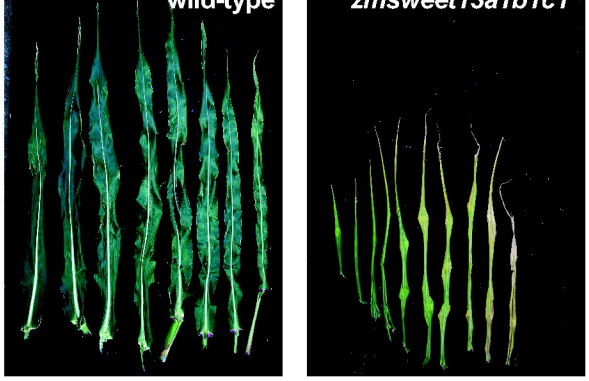
wild-type
zmsweet13a1b1c1

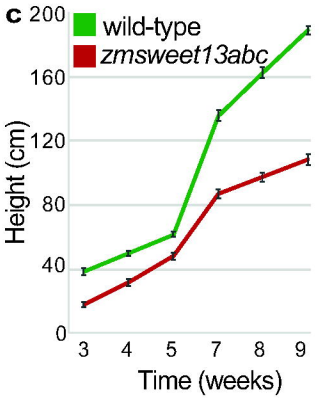
c
wild-type
zmsweet13abc
Height (cm)
0
40
80
120
160
200
3
4
5
7
8
9
Time (weeks)

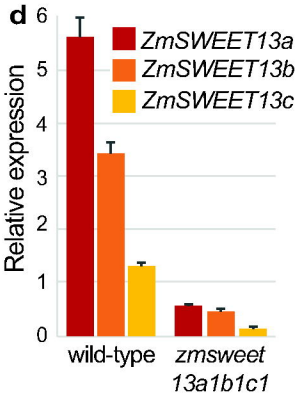
d
ZmSWEET13a
ZmSWEET13b
ZmSWEET13c
Relative expression
0
1
2
3
4
5
6
wild-type
zmsweet 13a1b1c1

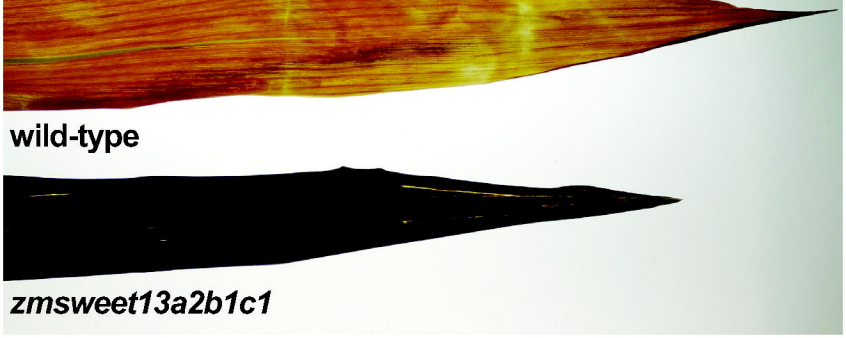
wild-type
zmsweet13a2b1c1

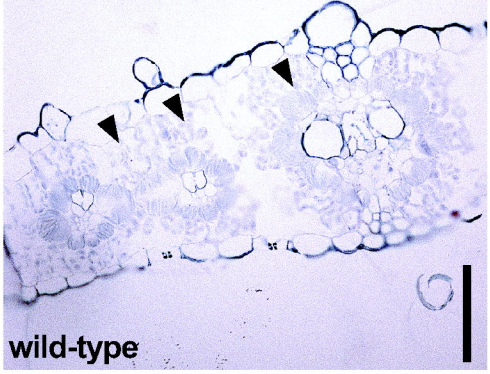
wild-type

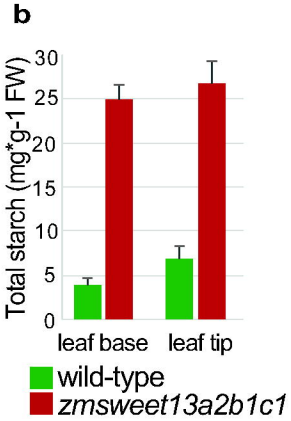
b
Total starch (mg*g-1 FW)
30
25
20
15
10
5
0
leaf base
leaf tip
wild-type
zmsweet13a2b1c1

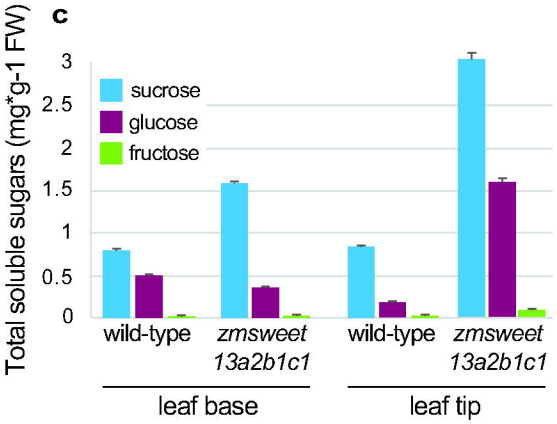
c
Total soluble sugars (mg*g-1 FW)
3
2.5
2
1.5
1
0.5
0
sucrose
glucose
fructose
wild-type
zmsweet 13a2b1c1
wild-type
zmsweet 13a2b1c1
leaf base
leaf tip

e
zmsweet13a2b1c1